

# Dynamic Dark Energy Equation of State (EoS) and Hubble Constant analysis using type Ia supernovae from Union 2.1 dataset.

Syed Faisal ur Rahman<sup>1</sup>★

<sup>1</sup> *Institute of Space and Planetary Astrophysics (ISPA), University of Karachi (UoK), Karachi, Pakistan*

Accepted XXX. Received YYY; in original form ZZZ

## ABSTRACT

This paper constraints dynamic dark energy equation of state (EoS) parameters using the type Ia supernovae from Union 2.1 dataset. The paper also discusses the dependency of dynamic dark energy EoS parameters on the chosen or assumed value of the Hubble Constant. To understand the correlation between the Hubble Constant values and measured dynamic dark energy EoS parameters, we used recent surveys being done through various techniques such as cosmic microwave background studies, gravitational waves, baryonic acoustic oscillations and standard candles to set values for different Hubble Constant values as fixed parameters with CPL and WCDM models. Then we applied trust region reflective (TRF) and dog leg (dogbox) algorithms to fit dark energy density parameter and dynamic dark energy EoS parameters. We found a significant negative correlation between the fixed Hubble Constant parameter and measured EoS parameter,  $w_0$ . Then we used two best fit Hubble Constant values (70 and 69.18474)  $\text{km s}^{-1} \text{Mpc}^{-1}$  based on Chi-square test to test more dark energy EoS parameters like: JBP, BA, PADE-I, PADE-II, and LH4 models and compared the results with  $\Lambda$ -CDM with constant  $w_{de}=-1$ , WCDM and CPL models. We conclude that flat  $\Lambda$ -CDM and WCDM models clearly provide best results while using the BIC criteria as it severely penalizes the use of extra parameters. However, the dependency of EoS parameters on Hubble Constant value and the increasing tension in the measurement of Hubble Constant values using different techniques warrants further investigation into looking for optimal dynamic dark energy EoS models to optimally model the relation between the expansion rate and evolution of dark energy in our universe.

**Key words:** Dark Energy EoS – Type Ia supernovae – Hubble Constant

## 1 INTRODUCTION

The discovery of the accelerated expansion of the universe (Riess et al. (1998) Perlmutter (1999) Perlmutter & Schmidt (2003)) revolutionized modern cosmology and answered many questions related to the evolution of our universe. However, we are still trying to understand the ingredient which is likely responsible for the accelerated expansion of the universe i.e. dark energy. Dark energy seems to be something which is not only overcoming the tendency of collapse of the matter in our universe but it is also providing a push for the accelerated expansion of our universe (Weinberg (2008)). After the discovery of the accelerated expansion of the universe in the late 1990s by

HighZ Supernova and the Supernova Cosmology Project teams (Riess et al. (1998) Perlmutter (1999) Perlmutter & Schmidt (2003)) using the type Ia supernovae, several observations applying various signatures like cosmic microwave background radiation (CMB), baryonic acoustic oscillation (BAO), Cepheid Variables, large scale structures etc. (Bennett et al. (2013) Hinshaw et al. (2013) Planck (2018) Birrer et al. (2018) Macaulay et al. (2019) Riess et al. (2019)), confirmed the accelerated expansion of our universe. Although, these observations confirm that our universe is going through a phase of accelerated expansion but these different observations also presented some serious problems by getting variations in their measurements of the cosmological parameters based on the standard model of cosmology or the  $\Lambda$ -CDM model (Liddle (2003) Jackson (2015) Rahman (2018)) which is providing impetus towards the development

★ E-mail: faisalrahman36@hotmail.com

of greater interest in non *Lambda*-CDM model studies (Zhai et al. (2017) Khosravi et al. (2019) Soli et al. (2019)). New standard candles like active galactic nuclei (AGN) are also being explored to get better measurements of cosmological parameters at high redshifts (Watson et al. (2011)).

## 2 COSMOLOGY FROM TYPE IA SUPERNOVA

Type Ia Supernovae are useful tools to be used as standard candles because of their almost standard absolute magnitude values. Therefore observations of apparent magnitude ( $m$ ) and redshift ( $z$ ) for type Ia Supernovae can lead to measurements of key cosmological parameters:  $\Omega_\Lambda$ ,  $\Omega_r$ , and  $\Omega_m$ , the dark energy, radiation and matter density parameters respectively within the *Lambda*-CDM cosmology framework. The difference between apparent magnitude ( $m$ ) and absolute magnitude is known as the distance modulus,  $\hat{A}_t$ :

$$\mu = m - M \quad (1)$$

Given a set of assumed cosmological parameters ( $C$ ), the redshift of an object, its apparent magnitude and luminosity distance  $DL$  are linked thus:

$$m(C, z) = 5 \log(DL(C, z)) + M + 25 \quad (2)$$

Thus luminosity distance and distance modulus are linked:

$$\mu(C, z) = 5 \log[DL(C, z)] + 25 \quad (3)$$

For a spatially flat universe, we can write luminosity distance as:

$$DL(z) = (1 + z)\chi(z) \quad (4)$$

Where,

$$\chi(z) = c\eta(z)$$

is the comoving distance and  $\eta(z)$  is conformal loop back time which can be calculated as:

$$\eta(z) = \int_0^z \frac{dz'}{H(z')} \quad (5)$$

Here,  $E(z) = \sqrt{\Omega_\Lambda I(z) + \Omega_r(1+z)^2 + \Omega_m(1+z)^3}$  for flat *Lambda*-CDM model.  $I(z)$  depends on the parametrization of the dark energy equation of state (EoS) and for standard *Lambda*-CDM model with EoS as  $w_{de}(z) = -1$  (constant), the multiplier  $I(z)$  becomes  $\hat{A}_t$ .

## 3 DATASET AND DATA ANALYSIS TECHNIQUES

For our study, we use Union 2.1 (Suzuki et al. (2012)) dataset publicly shared by Supernova Cosmology Project (SCP) (Perlmutter (1999) Perlmutter & Schmidt (2003) Amanullah et al. (2010)). The dataset is comprised of 580 type Ia supernovae which passed the usability cuts. The dataset is comprised of redshift range  $0.015 \leq z \leq 1.414$  with median redshift at  $z \approx 0.294$ .

We use SciPy's (Jones et al. (2001)) optimize package's trust region reflective (TRF) and dog leg (dogbox) algorithms (Vogl & Lagaris (2004)), which are suitable for problems with constraints as in our case, to fit dark energy

density parameter and dynamic dark energy EoS parameters for *Lambda*-CDM, WCDM, CPL, JBP, BA, PADE-I, PADE-II and LH4 models (Barboza & Alcaniz (2008) Chevallier & Polarski 2001 (2001) Linder (2003) Jassal et al. (2005a) Jassal et al. (2005b) Linder & Huterer (2005) Wei et al. (2014)). We also apply grid method to obtain maximum likelihood (Davis & Parkinson (2016)) for WCDM and CPL to compare results obtained through TRF and dog leg methods (Vogl & Lagaris (2004)). We used TRF and dogbox options simultaneously with our selected models and then used the best fit results based on the  $\chi^2$  values.

## 4 DYNAMIC DARK ENERGY EQUATION OF STATE (EOS)

$$I(z) = \exp\left(3 \int_0^z \frac{1 + w_{de}(z')}{1 + z'} dz'\right) \quad (6)$$

In order to extend the standard *Lambda*-CDM model to incorporate dynamic dark energy EoS, we can define  $I(z)$  as:

For the study we tested various dynamic dark energy EoS models.

We started with standard flat *Lambda*-CDM model with  $w_{de} = -1$  and then tested WCDM model by treating  $w_{de}$  as free parameter. Then we moved towards more complex CPL, JBP, BA, PADE-I, PADE-II and LH4 models (Barboza & Alcaniz (2008) Chevallier & Polarski 2001 (2001) Linder (2003) Jassal et al. (2005a) Jassal et al. (2005b) Linder & Huterer (2005) Wei et al. (2014)) with model equations as:

CPL (Chevallier & Polarski 2001 (2001) Linder (2003))

$$w_{de}(z) = w_0 + w_a \frac{z}{(1+z)} \quad (7)$$

JBP (Jassal et al. (2005a) Jassal et al. (2005b))

$$w_{de}(z) = w_0 + w_a \frac{z}{(1+z)^2} \quad (8)$$

BA (Barboza & Alcaniz (2008))

$$w_{de}(z) = w_0 + w_a \frac{z(1+z)}{(1+z^2)} \quad (9)$$

PADE-I (Wei et al. (2014))

$$w_{de}(z) = \frac{w_0 + w_a \frac{z}{(1+z)}}{1 + w_b \frac{z}{(1+z)}} \quad (10)$$

For  $w_b = 0$ , PADE-I reduces to CPL model.

PADE-II (Wei et al. (2014))

$$w_{de}(z) = \frac{w_0 + w_a \ln\left(\frac{1}{1+z}\right)}{1 + w_b \ln\left(\frac{1}{1+z}\right)} \quad (11)$$

Linder-Huterer (LH4) (Linder & Huterer (2005))

$$w_{de}(z) = w_0 + \frac{(w_a - w_0)}{1 + \frac{1}{(1+z)^{a_t}}} \quad (12)$$

For parameter boundaries for TRF and dog leg analysis, we set  $\Omega_\Lambda$  boundary between 0.65 and 0.75. For  $w_0$ , we

set the upper boundary as  $w_0 < -1/3$  which is a pre-condition for accelerated expansion of our universe but for lower limits we first set restrict it to  $w_0 \geq -1$  to exclude phantom dark energy (Vikman (2005) Farnes (2018)) and keeping it in quintessence regime (Weinberg (2008)). Then we set as  $\infty < w_0 \leq -1/3$  to allow phantom dark energy. This was done to minimize boundary condition bias while running the optimization algorithms. Similarly for  $w_a$ , we chose two set of boundaries  $-5 \leq w_a \leq 5$  and  $-0.3 \leq w_a \leq 0.3$  to avoid localization bias for optimization algorithm. In case of PADE I and II,  $w_b$  boundaries are set as  $-1 < w_b < 0$  while others remain same. In LH4 case, we set both  $T$  and  $a_t$  between 0 and 1.

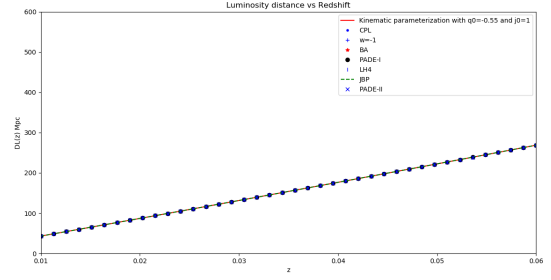


Figure 1.

## 5 HUBBLE CONSTANT VALUE

The value of Hubble Constant has recently been a topic of great interest in physics and astronomy community. It had been studied in the past like the first precise measurements by Sandage 1958 (Sandage (1958)) which gave  $H_0=75$  but recent interest has increased as the measurements of  $H_0$  from cosmic microwave background (CMB), baryon acoustic oscillations (BAO), standard candles and others do not seem to agree with each other (Freedman (2017) Jackson (2015) Planck (2018) Wojtak & Adriano 2019 (2019) Vattis et al. (2019) Riess et al. (2019)). The problem has become even more interesting as the expansion rate is found to be same in all directions by Soltis et al. 2019 based on 1000 type Ia supernovae sample. (Soltis et al. (2019)) Therefore we considered it appropriate to measure CPL and WCDM model parameters by fixing  $H_0$  values from Planck 2018, Riess 2018, Abbott et al. 2017, Planck+SNe+BAO-Planck 2018, Planck+BAO/RSD+WL-Planck 2018, H0LiCOW 2018 and DES 2018 (Abbott et al. (2017) Birrer et al. (2018)). We also fit our own value for Union 2.1 dataset (Suzuki et al. (2012)) using the kinematic expression from Riess et al. 2016 (Riess et al. (2016)) for luminosity distance with source redshift of  $z < 0.04$ . Figure 1 shows that luminosity distances from (13) is in good agreement with luminosity distances from (4) for  $z < 0.04$  using various EoS models.

The kinematic expression from Riess et al. 2016 is written as:

$$DL(z) = \frac{cz}{H_0} \left[ 1 + \frac{(1-q_0)z}{2} - \frac{(1-q_0-3q_0^2+j_0)z^2}{6} + O(z^3) \right] \quad (13)$$

With  $q_0 = -0.55$  and  $j_0 = 1$ .

We can see from tables 1 and 2 that our best measurements based on  $\chi^2$  values for both CPL and WCDM are obtained through  $H_0=70 \text{ km s}^{-1} \text{ Mpc}^{-1}$  which is measured by Abbott et al. 2017 by studying gravitational waves (GW170817) (LIGO (2017) Abbott et al. (2016) Abbott et al. (2017)) from neutron stars collision and was also measured by Wilkinson Microwave Anisotropy Probe (WMAP) (Bennett et al. (2013)) with WMAP only dataset. Our second best measurements were obtained through the best fit  $H_0=69.18473827 \pm 0.50179901$  or approximately  $69.185 \text{ km s}^{-1} \text{ Mpc}^{-1}$  value from Union 2.1 dataset using kinematic expression for luminosity distance which is closer to the value obtained by (Bennett et al. (2013)) using WMAP+eCMB+BAO+ $H_0$  data set (Hinshaw et al.

Table 1. Add caption

| WCDM          |                 |                |                 |  |
|---------------|-----------------|----------------|-----------------|--|
| $H_0$         | $\Omega\Lambda$ | $w_0$          | $\chi^2$        | Bounds on $\Omega\Lambda, w_0$                   |
| 67.400        | 0.75            | -0.7024        | 606.6761        | (0.65,0.75), $(-\infty, -1/3)$                   |
| 67.400        | 0.75            | -0.7024        | 606.6761        | (0.65,0.75), $(-1, -1/3)$                        |
| 73.520        | 0.65            | -1.7459        | 614.5908        | (0.65,0.75), $(-\infty, -1/3)$                   |
| 73.520        | 0.75            | -1.0000        | 740.6163        | (0.65,0.75), $(-1, -1/3)$                        |
| <b>70.000</b> | <b>0.72</b>     | <b>-1.0045</b> | <b>562.2257</b> | <b>(0.65,0.75), <math>(-\infty, -1/3)</math></b> |
| 70.000        | 0.72            | -1.0000        | 562.2267        | (0.65,0.75), $(-1, -1/3)$                        |
| 72.500        | 0.65            | -1.5683        | 588.7033        | (0.65,0.75), $(-\infty, -1/3)$                   |
| 72.500        | 0.75            | -1.0000        | 646.1989        | (0.65,0.75), $(-1, -1/3)$                        |
| 67.770        | 0.75            | -0.7353        | 594.2718        | (0.65,0.75), $(-\infty, -1/3)$                   |
| 67.770        | 0.75            | -0.7353        | 594.2718        | (0.65,0.75), $(-1, -1/3)$                        |
| <b>69.185</b> | <b>0.75</b>     | <b>-0.8645</b> | <b>565.9402</b> | <b>(0.65,0.75), <math>(-\infty, -1/3)</math></b> |
| <b>69.185</b> | <b>0.75</b>     | <b>-0.8645</b> | <b>565.9402</b> | <b>(0.65,0.75), <math>(-1, -1/3)</math></b>      |

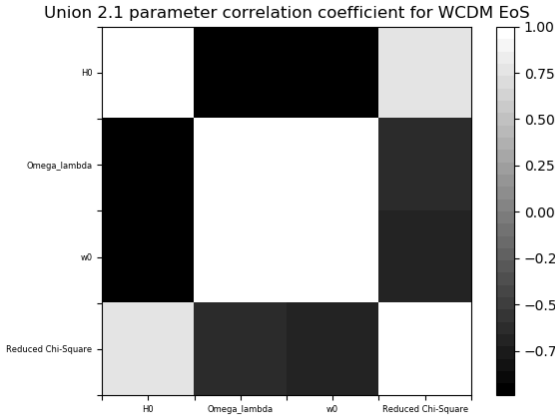
(2013)). We applied TRF with bounds  $65 \leq H_0 \leq 75$  to obtain the best fit  $H_0$  value. Both of these values are interestingly somewhat in the middle region of the  $H_0$  values obtained by early universe studies (Gorbunov & Rubakov (2011)) like Planck cosmic microwave background (CMB) (Planck (2014a) Planck (2014b) Planck (2016) Planck (2018)) or baryon acoustic oscillations (BAO) (Grieb et al. (2017), Macaulay et al. (2019)) which give  $H_0 \approx 67$  and standard candles studies like (Riess et al. (1998) Riess et al. (2007) Riess et al. (2016) Riess et al. 2018a (2018a) Riess et al. (2018b) Pietrzyński et al. (2019) Riess et al. (2019)) which give  $H_0 > 73$ . Because of this discrepancy in the measurement of  $H_0$ , higher redshift studies of type Ia supernovae and other standard candles are becoming important (Risaliti & Lusso 2019 (2019) Riess et al. 2018a (2018a) Daniel et al. (2019)). Like early universe studies, standard candles are also useful to study the nature of dark energy (Wood-Vasey et al. (2007)) which is still an open problem of cosmology (Davis et al. (2007) Davis & Parkinson (2016)).

In order to understand how  $H_0$  value affects the measurements of dynamic dark energy EoS model parameters, we simply cross-correlated the data in tables 1 and 2. Figures 2 and 3 show how the measurement or choice of the Hubble Constant can affect the measurements of dynamic dark energy EoS parameters in WCDM and CPL models. We can clearly observe significant negative cross-correlation between  $w_0$  and  $H_0$  for both WCDM and CPL models.

These results are particularly interesting due to the Hubble Constant tension arising due to the differences in

**Table 2.** Best fit values for CPL model using union 2.1 dataset

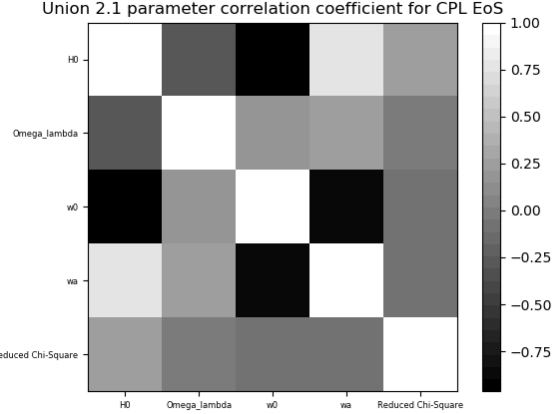
| CPL           |                 |               |               |                 |  |
|---------------|-----------------|---------------|---------------|-----------------|--|
| H0            | $\Omega\Lambda$ | w0            | wa            | $\chi^2$        | Bounds on $\Omega\Lambda, w0, wa$        |
| 66.300        | 0.65            | -0.333        | -3.601        | <b>620.9512</b> | (0.65, 0.75), (-∞, -1/3), (-5, 5)        |
| 66.300        | 0.65            | -0.333        | -3.601        | <b>620.9512</b> | (0.65, 0.75), (-1, -1/3), (-5, 5)        |
| 66.300        | 0.75            | -0.567        | -0.300        | <b>650.2256</b> | (0.65, 0.75), (-∞, -1/3), (-0.3, 0.3)    |
| 66.300        | 0.75            | -0.567        | -0.300        | <b>650.2256</b> | (0.65, 0.75), (-1, -1/3), (-0.3, 0.3)    |
| 67.400        | 0.65            | -0.333        | -4.678        | <b>585.7344</b> | (0.65, 0.75), (-∞, -1/3), (-5, 5)        |
| 67.400        | 0.65            | -0.333        | -4.678        | <b>585.7344</b> | (0.65, 0.75), (-1, -1/3), (-5, 5)        |
| 67.400        | 0.75            | -0.664        | -0.300        | <b>602.6112</b> | (0.65, 0.75), (-∞, -1/3), (-0.3, 0.3)    |
| 67.400        | 0.75            | -0.664        | -0.300        | <b>602.6112</b> | (0.65, 0.75), (-1, -1/3), (-0.3, 0.3)    |
| 67.770        | 0.65            | -0.419        | -4.326        | <b>579.2176</b> | (0.65, 0.75), (-∞, -1/3), (-5, 5)        |
| 67.770        | 0.65            | -0.419        | -4.326        | <b>579.2176</b> | (0.65, 0.75), (-1, -1/3), (-5, 5)        |
| 67.770        | 0.75            | -0.697        | -0.300        | <b>590.9692</b> | (0.65, 0.75), (-∞, -1/3), (-0.3, 0.3)    |
| 67.770        | 0.75            | -0.697        | -0.300        | <b>590.9692</b> | (0.65, 0.75), (-1, -1/3), (-0.3, 0.3)    |
| 68.340        | 0.65            | -0.584        | -3.491        | <b>571.3333</b> | (0.65, 0.75), (-∞, -1/3), (-5, 5)        |
| 68.340        | 0.65            | -0.584        | -3.491        | <b>571.3333</b> | (0.65, 0.75), (-1, -1/3), (-5, 5)        |
| 68.340        | 0.75            | -0.749        | -0.300        | <b>577.1210</b> | (0.65, 0.75), (-∞, -1/3), (-0.3, 0.3)    |
| 68.340        | 0.75            | -0.749        | -0.300        | <b>577.1210</b> | (0.65, 0.75), (-1, -1/3), (-0.3, 0.3)    |
| <b>69.185</b> | <b>0.65</b>     | <b>-0.830</b> | <b>-2.278</b> | <b>564.2394</b> | <b>(0.65, 0.75), (-∞, -1/3), (-5, 5)</b> |
| <b>69.185</b> | <b>0.65</b>     | <b>-0.830</b> | <b>-2.278</b> | <b>564.2394</b> | <b>(0.65, 0.75), (-1, -1/3), (-5, 5)</b> |
| 69.185        | 0.75            | -0.827        | -0.300        | <b>565.2861</b> | (0.65, 0.75), (-∞, -1/3), (-0.3, 0.3)    |
| 69.185        | 0.75            | -0.827        | -0.300        | <b>565.2861</b> | (0.65, 0.75), (-1, -1/3), (-0.3, 0.3)    |
| <b>70.000</b> | <b>0.72</b>     | <b>-1.005</b> | <b>-0.011</b> | <b>562.2257</b> | <b>(0.65, 0.75), (-∞, -1/3), (-5, 5)</b> |
| <b>70.000</b> | <b>0.72</b>     | <b>-1.005</b> | <b>-0.011</b> | <b>562.2257</b> | <b>(0.65, 0.75), (-1, -1/3), (-5, 5)</b> |
| 70.000        | 0.72            | -1.000        | 0.039         | <b>562.2260</b> | (0.65, 0.75), (-∞, -1/3), (-0.3, 0.3)    |
| 70.000        | 0.72            | -1.000        | 0.039         | <b>562.2260</b> | (0.65, 0.75), (-1, -1/3), (-0.3, 0.3)    |
| 72.500        | 0.67            | -1.727        | 2.402         | <b>583.9811</b> | (0.65, 0.75), (-∞, -1/3), (-5, 5)        |
| 72.500        | 0.65            | -1.598        | 0.300         | <b>587.6217</b> | (0.65, 0.75), (-∞, -1/3), (-0.3, 0.3)    |
| 72.500        | 0.75            | -1.000        | -1.142        | <b>623.7469</b> | (0.65, 0.75), (-1, -1/3), (-5, 5)        |
| 72.500        | 0.75            | -1.000        | -0.300        | <b>635.4969</b> | (0.65, 0.75), (-1, -1/3), (-0.3, 0.3)    |
| 73.520        | 0.65            | -2.101        | 3.575         | <b>603.5328</b> | (0.65, 0.75), (-∞, -1/3), (-5, 5)        |
| 73.520        | 0.65            | -1.773        | 0.300         | <b>613.0368</b> | (0.65, 0.75), (-∞, -1/3), (-0.3, 0.3)    |
| 73.520        | 0.75            | -1.000        | -1.950        | <b>682.8480</b> | (0.65, 0.75), (-1, -1/3), (-5, 5)        |
| 73.520        | 0.75            | -1.000        | -0.300        | <b>722.6496</b> | (0.65, 0.75), (-1, -1/3), (-0.3, 0.3)    |

**Figure 2.** Cross-correlation of WCDM model parameters with H0,  $\chi^2$  and each other. We can clearly observe significant negative cross-correlation between w0 and H0.

measurements of H0 through cosmic microwave background, standard candles and other techniques.

## 6 RESULTS

In figure 4, for WCDM model, the maximum likelihood fit values are  $\Omega\Lambda = 0.712^{+0.039}_{-0.021}$  and  $w0 = -0.995^{+0.070}_{-0.073}$ . Their corresponding mean likelihood fit values are  $\Omega\Lambda = 0.724 \hat{\pm} 0.030$  and  $w0 = -1 \hat{\pm} 0.065$ . Both maximum and mean like-

**Figure 3.** Cross-correlation of CPL model parameters with H0,  $\Omega\Lambda$ , w0, wa and each other. We can again clearly observe significant negative cross-correlation between w0 and H0. We can also observe positive cross-correlation between H0 and wa.

likelihood values agree, within one sigma overlapping values, with the best fit values obtained by using TRF and dog leg methods for H0=70. The best values from from tables 1 and 8 are  $\Omega\Lambda = 0.720362 \hat{\pm} 0.0626$  and  $w0 = -1.00449 \hat{\pm} 0.1435$ . Values in table 1 are rounded off to fit in the columns.

In figure 5, for WCDM model, the maximum likelihood fit values are  $\Omega\Lambda = 0.687^{+0.103}_{-0.060}$ ,  $w0 = -0.98^{+0.014}_{-0.014}$  and  $wa = -0.35^{+0.47}_{-0.92}$ . Their corresponding mean likelihood fit values are  $\Omega\Lambda = 0.731 \hat{\pm} 0.080$ ,  $w0 = -1.02 \hat{\pm} 0.015$  and  $wa = 0.01 \hat{\pm} 0.65$ . Again both maximum and mean likelihood values agree, within one sigma overlapping values, with the best fit values obtained by using TRF and dog leg methods for H0=70. The best values from from tables 2 and 8 are  $\Omega\Lambda = 0.71933 \hat{\pm} 0.27885$ ,  $w0 = -1.00547 \hat{\pm} 0.291303$  and  $wa = -0.01126 \hat{\pm} 3.033239$ . Values in table 1 are rounded off to fit in the columns. For wa, there is a relatively larger standard deviation in both likelihood estimates and in TRF and dog leg optimization approaches which is likely due to smaller redshift coverage from type Ia supernovae sample from Union 2.1. On very large redshifts, wa almost plays an equal role as w0 in CPL model because on extremely large 'z' values,  $w_{de}(z)$  approximately becomes  $w0 + wa$ . However in case of a model like JBP, the model will be more or entirely dependent on w0. This means higher redshift surveys especially highly sensitive all sky surveys like galaxy surveys to study the late time integrated Sachs-Wolfe effect (ISW) (Sachs & Wolfe 1967 (1967) Afshordi (2004) Rahman & Iqbal 2019 (2019)) or surveys studying the early universe signatures like cosmic microwave background radiation (CMB) or baryonic acoustic oscillations (BAO), can play an important part in estimating parameters like wa or other extended EoS model parameters can make major contributions in higher redshifts in various dynamic dark energy equation of state (EoS) models which are in discussion in this study.

To see how dynamic dark energy EoS evolves in JBP, BA, PADE-I, PADE-II, and LH4 models especially in comparison the results from the flat  $\Lambda$ -CDM model with constant  $w_{de} = -1$ , WCDM and CPL models, we again applied

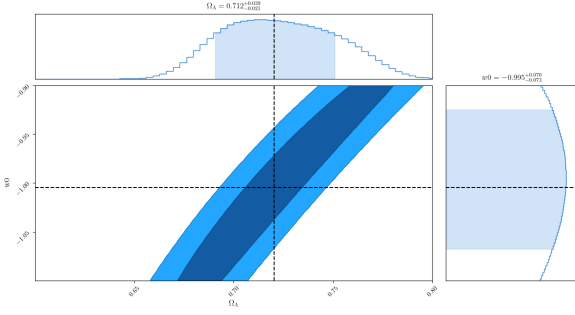


**Figure 4.** WCDM parameter constraints obtained through maximum likelihood and comparison with results from TRF and dog leg methods (dark dashed lines).

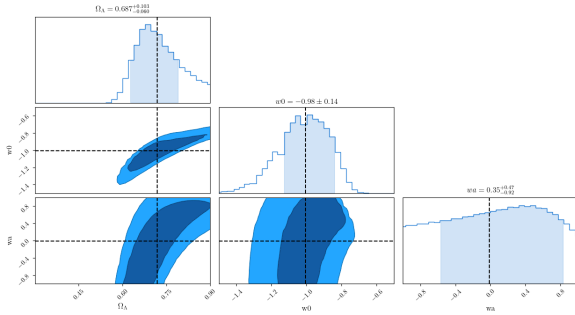


**Figure 5.** CPL parameter constraints obtained through maximum likelihood and comparison with results from TRF and dog leg methods (dark dashed lines).

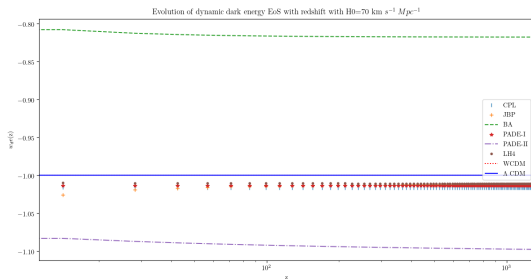


**Figure 6.** Evolution of  $w_{de}(z)$  for various dynamic dark energy EoS models with redshift for  $H_0=70 \text{ km s}^{-1} \text{ Mpc}^{-1}$ .

TRF and dog leg methods (Voglís & Lagaris (2004)) simultaneously and selected the best fit values based on  $\chi^2$  criteria.

We can see in figure 6 that for  $H_0=70 \text{ km s}^{-1} \text{ Mpc}^{-1}$ , the results are closer to  $\Lambda$ -CDM model with constant  $w_{de}=-1$  except for BA model which is in quintessence regime and PADE-II which is a bit farther than  $w_{de}=-1$  in comparison with others. However, due to large standard deviations from mean for  $w_a$ ,  $w_b$ ,  $a_t$  and  $T$  parameters in CPL, JBP, BA, PADE-I, PADE-II and LH4 models (Barboza & Alcaniz (2008) Chevallier & Polarski 2001 (2001) Linder (2003) Jassal et al. (2005a) Jassal et al. (2005b) Linder & Huterer (2005)

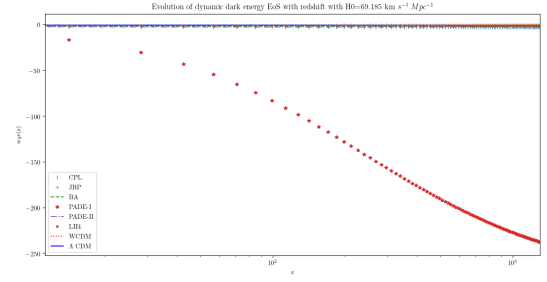


**Figure 7.** Evolution of  $w_{de}(z)$  for various dynamic dark energy EoS models with redshift for  $H_0=69.185 \text{ km s}^{-1} \text{ Mpc}^{-1}$ .

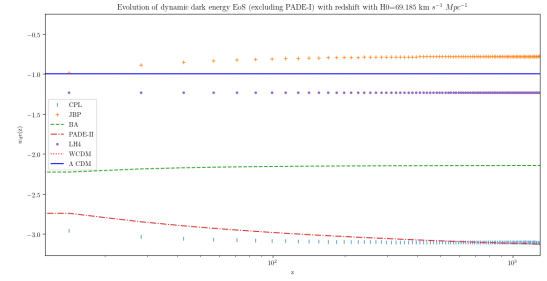


**Figure 8.** Evolution of  $w_{de}(z)$  for various dynamic dark energy EoS models with redshift for  $H_0=69.185 \text{ km s}^{-1} \text{ Mpc}^{-1}$  excluding PADE-I.

Wei et al. (2014)) for relatively smaller redshift objects like in Union 2.1 dataset of type Ia supernovae, we still need to test these models using early universe signatures like CMB and BAO. For our type Ia supernova dataset with relatively smaller redshift coverage in comparison with they early universe studies, we can see that  $\Lambda$ -CDM model with  $w_{de}=-1$  as fixed value is still the preferred model based on Bayesian information criterion (BIC) (Schwarz (1978) Arevalo et al. (2017) Liddle 2007 (2007)) especially if we consider  $\Delta\text{BIC}$  values which are basically the difference of BIC values from our models in discussion with the lowest BIC obtained from these models.  $\Delta\text{BIC} > 2$  suggests positive evidence against a model with higher BIC and  $\Delta\text{BIC} > 6$  suggests strong evidence against higher BIC value models (Kass & Raftery (1995)) as BIC heavily penalizes the inclusion of newer parameters (Liddle 2007 (2007)) despite having better  $\chi^2$  scores for non  $\Lambda$ -CDM models. This can change for higher redshift or early universe studies when extra parameters in dynamic dark energy EoS models are potentially going to play important role which will also be useful for  $H_0$  studies (Gorbunov & Rubakov (2011) Planck (2018) Riess et al. (2019) Risaliti & Lusso 2019 (2019) Poulin et al. (2019) Liu et al. (2019)) .

For  $H_0=69.185 \text{ km s}^{-1} \text{ Mpc}^{-1}$ , we first look at figure 7 and observe that PADE-I is showing most deviation from  $w_{de}=-1$  in comparison with the others especially at higher redshifts. This difference in scale of deviation towards  $w_{de}=-1$  is due to the relatively higher contribution of  $w_a$  and  $w_b$  of PADE-I model with increasing redshift values. In figure 8, we



remove PADE-I model to see the evolution of  $w_{de}(z)$  in other models. We can see that apart from JBP, which is moving towards quintessence regime, others are closer to phantom regime (Vikman (2005) Farnes (2018)) with BA and PADE-II deviating away more from  $w_{de}=-1$  and towards phantom regime. Theoretically, all structures in our universe would be eventually ripped apart by the repulsive force associated with the phantom dark energy (Vikman (2005) Weinberg (2008)). It will be interesting to see if future high precision standard candles, early universe and other surveys can settle expansion rate debate and which  $w_{de}$  evolution or best fit value will be associated with it as we can observe from figures 2 and 3 that expansion rate and dark energy EoS parameters have significant cross-correlation with each other.

We can also see from figures 6, 7 and 8 that despite  $H_0$  values being  $< 2\%$  different from each other, their impact on  $w_{de}(z)$  evolution is significant for all the models. This difference is significant enough to impact our understanding of the scales and evolution of our universe which warrants the need to carefully model  $w_{de}(z)$  in observations of early universe signatures, galaxy surveys, standard candles, standard rulers and recently discovered gravitational waves which can be used as standard sirens (Schutz (1999) Jarvis et al. (2014) Rahman (2018) Chen et al. (2018)). Gravitational waves can also be used to study the gravitational wave strain signals from type Ia supernovae and we can use them to study cosmological parameters. For this purpose it will be useful to carefully study the progenitors of the type Ia supernovae (Keiichi & Terada 2016 (2016) Rahman (2018)) as the mass profiles of the objects involved will be crucial in modeling the expected signal (Schutz (1999) Rahman (2018)).

## 7 CONCLUSION

We studied various dynamic dark energy EoS models and also discussed the key EoS parameter  $w_0$  in relation with the Hubble Constant. We also observed strong negative correlation between the Hubble Constant and EoS parameter  $w_0$ . This relation is also studied in relation with different  $H_0$  values obtained from various surveys adopting different techniques to constraint the cosmological parameters especially  $H_0$ . We found that the models we tested agreed mostly with standard cosmological model predictions. We also observed that the extended dynamic dark energy equation of state (EoS) models we tested agreed with the idea of a universe going through an accelerated expansion phase. We also observed that the value of  $w_0$ , which provides value of  $w_{de}(z)$  at  $z=0$  or the current epoch, is in quite close to the standard  $\Lambda$ -CDM constant value of  $w_{de}=-1$  with  $w_0=-1$  in the confidence interval of one sigma. For the Hubble Constant value of  $H_0 \approx 69.185$ , which we fit on Union 2.1 dataset using kinematic expression for luminosity distance, we found that best fit values for dynamic dark energy EoS models deviate from the constant  $w_{de}=-1$ . However,  $\Lambda$ -CDM with constant value of  $w_{de}=-1$  still comes as the preferable model based on the BIC selection criteria. However this deviation, even in the EoS models with higher number of parameters, shows the importance of studying  $H_0$  in relation with  $w_{de}(z)$ . Based on our results, we can also conclude that by carefully modeling and studying  $w_{de}(z)$ , we can potentially resolve the

Hubble Constant tension arising from the results obtained using different techniques.

## 8 ACKNOWLEDGEMENT

I would like to thank Prof. Dr. Jeremy Mould, Emeritus Professor at Swinburne University of Technology for reviewing this work and providing useful suggestions during the development of this paper.

**Table 3.** Best Fit Parameters for Dynamic Dark Energy EoS models using Union 2.1 SN type Ia Dataset

| Hubble Constant $H_0$ | EoS Models                            | $\Omega_{\text{m}}$ , $\Lambda_{\text{m}}$ | $w_0$                     | Parameter Values         | $w_b$                   | $a_1$                    | T                       | Chi-Square | Para | BIC      |
|-----------------------|---------------------------------------|--|---------------------------|--------------------------|-------------------------|--------------------------|-------------------------|------------|------|----------|
| <b>70(Fixed)</b>      |                                       |  |                           |                          |                         |                          |                         |            |      |          |
|                       | $\Lambda$ -CDM ( $w_{\text{de}}=-1$ ) | 0.722287 $\pm$ 0.013                       | -1                        |                          |                         |                          |                         | 562.2267   | 1    | 568.5897 |
|                       | WCDM                                  | 0.720362 $\pm$ 0.0626                      | -1.00449 $\pm$ 0.1435     |                          |                         |                          |                         | 562.2257   | 2    | 574.9518 |
|                       | CPL                                   | 0.71913 $\pm$ 0.27885                      | -1.00547 $\pm$ 0.291305   | -0.01126 $\pm$ 3.033239  |                         |                          |                         | 562.2257   | 3    | 581.3148 |
|                       | JBP                                   | 0.70796 $\pm$ 0.17292                      | -1.011969 $\pm$ 0.1643    | -0.22393 $\pm$ 3.2172    |                         |                          |                         | 562.2219   | 3    | 581.311  |
|                       | RA                                    | 0.75 $\pm$ 0.86891                         | -0.9691 $\pm$ 1.06464     | 0.15139 $\pm$ 3.50097    |                         |                          |                         | 562.2117   | 3    | 581.308  |
|                       | PADE-I                                | 0.7196 $\pm$ 1.28324                       | -1.05123 $\pm$ 1.94515    | -0.00578414 $\pm$ 4909.4 | -0.002752 $\pm$ 4882.5  |                          |                         | 562.2257   | 4    | 587.6778 |
|                       | PADE-II                               | 0.712876 $\pm$ 0.4852                      | -1.01089 $\pm$ 0.7675     | 1.10857 $\pm$ 271.43     | -0.998715 $\pm$ 267.121 |                          |                         | 562.2249   | 4    | 587.6771 |
|                       | LH4                                   | 0.72007 $\pm$ 2.0615                       | -0.999102 $\pm$ 223.47    | -1.01078 $\pm$ 314.52    |                         | 0.9379244 $\pm$ 29648.86 | 0.960383 $\pm$ 39515.18 | 562.2258   | 5    | 594.0409 |
| <b>69.185(Fixed)</b>  |                                       |  |                           |                          |                         |                          |                         |            |      |          |
|                       | $\Lambda$ -CDM ( $w_{\text{de}}=-1$ ) | 0.68671517 $\pm$ 0.01366395                | -1                        |                          |                         |                          |                         | 567.9516   | 1    | 574.3546 |
|                       | WCDM                                  | 0.75 $\pm$ 0.08088                         | -0.86452 $\pm$ 0.1448     |                          |                         |                          |                         | 565.9402   | 2    | 578.6663 |
|                       | CPL                                   | 0.65 $\pm$ 0.094414                        | -0.82971 $\pm$ 0.112769   | -2.27778 $\pm$ 2.70177   |                         |                          |                         | 564.2394   | 3    | 583.3285 |
|                       | JBP                                   | 0.65 $\pm$ 0.08967                         | -0.77572 $\pm$ 0.13167    | -3.38651 $\pm$ 3.53197   |                         |                          |                         | 563.8489   | 3    | 582.918  |
|                       | RA                                    | 0.65 $\pm$ 0.10221                         | -0.88266 $\pm$ 0.1076     | -1.280134 $\pm$ 1.7388   |                         |                          |                         | 564.707    | 3    | 583.796  |
|                       | PADE-I                                | 0.66586 $\pm$ 0.12523                      | -0.88078055 $\pm$ 0.11613 | -0.299997 $\pm$ 2.02684  | -0.9958 $\pm$ 0.0000003 |                          |                         | 564.1249   | 4    | 589.577  |
|                       | PADE-II                               | 0.65 $\pm$ 0.2274                          | -0.81318 $\pm$ 0.5637     | 3.446955 $\pm$ 23.726    | -0.999 $\pm$ 20.04      |                          |                         | 564.1126   | 4    | 589.5647 |
|                       | LH4                                   | 0.65596 $\pm$ 0.05682                      | -0.38368 $\pm$ 0.71809    | -1.23068 $\pm$ 0.28266   |                         | 0.96887 $\pm$ 0.03171    | 0.000875 $\pm$ 0.26241  | 561.3055   | 5    | 593.1186 |

## REFERENCES

- Abbott B.P. et al., 2016, Phys.Rev.Lett. 116 no.6, 061102  
arXiv:1602.03837 [gr-qc] LIGO-P150914
- Abott B. P. et al. , 2017, Phys.Rev.Lett. 119, 161101
- Afshordi,2004, Phys. Rev. D,70,083536
- Amanullah et al., 2010, (The Supernova Cosmology Project),  
Astrophys.J.716:712-738
- Arevalo F., Cid A., Moya J., 2017, Eur. Phys. J. C 77: 565.  
<https://doi.org/10.1140/epjc/s10052-017-5128-7>
- Barboza Jr. E. M. , Alcaniz J.S., 2008, Phys. Rev. B 666 415
- Bennett C. L. et al., 2013, The Astrophysical Journal Supplement,  
Volume 208, Issue 2, article id. 20, 54 pp.
- Birrer S, Treu T, Rusu C. E, et al., 2018, Monthly Notices of the  
Royal Astronomical Society. 484(4): 4726-4753.
- Chen Hsin-Yu, Fishbach Maya, Holz Daniel E., 2018, Nature, Vol-  
ume 562, Issue 7728, p.545-547
- Chevallier M, Polarski D, 2001, Int. J. Mod. Phys. D 10, 213, [gr-  
qc/0009008
- Daniel S., Perlmutter S. et al., 2019, Astro2020: Decadal Survey  
on Astronomy and Astrophysics, science white papers, no.  
270, arXiv:1903.05128
- Davis T.M., Parkinson D., 2016, Characterizing Dark Energy  
Through Supernovae. In: Alsabti A., Murdin P. (eds) Hand-  
book of Supernovae. Springer, doi:10.1007/978-3-319-20794-  
0\_106-1
- Davis T.M., Årtur E., ESSENCE et al., 2007, The Astro-  
physical Journal, Volume 666, Issue 2, pp. 716-725., astro-  
ph/0701510
- Farnes J. S., 2018, Astronomy and Astrophysics. 620: A92
- Freedman Wendy L., 2017, Nature Astronomy, Volume 1, id. 0121
- Gorbunov S., Rubakov V.A. , 2011, Introduction to the The-  
ory of the Early Universe: Cosmological Perturbations and  
Inflationary Theory, World Scientific, Singapore
- Grieb Jan N., Sánchez Ariel G., Salazar-Albornoz Salvador,  
2017, Monthly Notices of the Royal Astronomical Society, Vol-  
ume 467, Issue 2, p.2085-2112
- Hinshaw G. et al., 2013, Astrophys. J.Suppl. Ser., 208,19
- Jackson N., 2015, Living Rev Relativ 18: 2.  
<https://doi.org/10.1007/lrr-2015-2>
- Jarvis M., Bacon D., Blake C. et al., 2014, SKA Cosmology  
Chapter, Advancing Astrophysics with the SKA (AASKA14)  
Conference, Giardini Naxos (Italy), June 9th-13th 2014,  
arXiv:1501.03825
- Jassal H.K., Bagla J.S., Padmanabhan T., 2005, MNRAS 356 L11
- Jassal H.K., Bagla J.S., Padmanabhan T., 2005b, Phys. Rev. D  
72 103503
- Jones E, Oliphant E, Peterson P, et al.,  
2001, <http://www.scipy.org/>
- Kass Robert E., Raftery Adrian E., 1995, Journal of  
the American Statistical Association, 90(430):  
773-795, doi:10.2307/2291091, ISSN 0162-  
1459, JSTOR 2291091
- Keiichi Maeda, Yukikatsu Terada, 2016, International Journal of  
Modern Physics D, Vol. 25, No. 10 1630024
- Khosravi Nima, Baghran Shant, Afshordi Niayesh, Altamirano  
Natacha, 2019, Physical Review D, Volume 99, Issue 10,  
id.103526
- Liddle A., 2003, "Introduction to modern Cosmology", Second  
edition, University of Sussex, UK, Wiley Publication
- Liddle A.R., 2007, Monthly Notices of the Royal Astronomical So-  
ciety: Letters, Volume 377, Issue 1, pp. L74-L78
- The LIGO Scientific Collaboration, The Virgo Collaboration, The  
1M2H Collaboration, The Dark Energy Camera GW-EM Col-  
laboration and the DES Collaboration, The DLT40 Collabora-  
tion, The Las Cumbres Observatory Collaboration, The VIN-  
ROUGE Collaboration, The MASTER Collaboration, Ab-  
bott et al., 2017, Nature. advance online publication (7678):  
85-88. arXiv:1710.05835
- Linder E. V., Huterer D., 2005, Phys. Rev. D 72, 043509
- Linder E. V., 2003, Phys. Rev. Lett., 90, 091301, [astro-  
ph/0311403]
- Bin Liu, Zhengxiang Li, Zong-Hong Zhu, 2019, Monthly Notices  
of the Royal Astronomical Society, Volume 487, Issue 2, Pages  
1980-1985, <https://doi.org/10.1093/mnras/stz1179>
- Macaulay E., Nichol R. C., Bacon D. et al.,  
2019, Monthly Notices of the Royal Astro-  
nomical Society, Volume 486, Issue 2, Pages  
2184-2196, <https://doi.org/10.1093/mnras/stz978>
- Perlmutter S., Schmidt B., 2003, Supernovae and Gamma Ray  
Bursts, K. Weiler, ed., Springer-Verlag, New York
- Perlmutter S., 1999, Astrophys. J. 517, 565
- PietrzyÅski G., Graczyk D., Gallenne A., et al. 2019, Nature,  
567, 200. <https://doi.org/10.1038/s41586-019-0999-4>
- Planck Collaboration, Bucher, P. A. R. et al., 2014, A&A 571:  
A1
- Planck Collaboration, P.A.R. Ade , et al., 2014 , A&A, Volume  
571, id.A23, 48 pp.
- Planck Collaboration, 2016, A&A 594, A1
- Planck Collaboration, 2018, [www.cosmos.esa.int](http://www.cosmos.esa.int). arXiv:1807.06209
- Poulin Vivian, Smith Tristan L., Karwal Tanvi, Kamionkowski  
Marc, 2019, Physical Review Letters, Volume 122, Issue 22,  
id.221301
- Rahman S.F., Iqbal M.J., 2019 ,Eur. Phys. J. Plus 134: 302.  
<https://doi.org/10.1140/epjp/i2019-12669-y>
- Rahman S.F. Astronomy & Geophysics, Volume 59, Issue 2, Pages  
2.39-2.42, 2018
- Riess et al., 1998, AJ Vol. 16
- Riess et al., 2007, Astrophys.J. 659 98-121 astro-ph/0611572  
4645850950
- Riess A. G., Macri L. M., Hoffmann S. L., et al. 2016, ApJ, 826,  
56
- Riess et al., 2018, The Astrophysical Journal, Volume 853, Issue  
2, article id. 126, 15 pp.
- Riess Adam G., Casertano Stefano, Yuan Wenlong et al., 2018,  
The Astrophysical Journal. 861(2): 126
- Riess Adam G., Casertano Stefano, Yuan Wenlong, Macri Lu-  
cas M., Scolnic, Dan, 2019, arXiv:1903.07603, ApJ ac-  
cepted 2019
- Risaliti G., Lusso E., 2019, Nature Astronomy volume 3,  
pages 272-277
- Sachs R.K., 1967, Wolfe A.M., Astrophys. J., 147, 73
- Sandage A. R., 1958, Astrophysical Journal, vol. 127, p.513
- Classical and Quantum Gravity, Volume 16, Number 12A
- Schwarz Gideon E. , 1978, Annals of Statistics, 6(2):  
461-464, doi:10.1214/aos/1176344136
- SolÀ Peracaula Joan, GÀmez-Valent AdriÀ, de Cruz PÀrez  
Javier, 2019, Physics of the Dark Universe, Volume 25, article  
id. 100311.
- Soltis J., Farahi A., Huterer D., Liberato C.M., 2019 ,Phys. Rev.  
Lett. 122, 091301
- Suzuki et al., 2012 (The Supernova Cosmology Project), The As-  
trophysical Journal, Volume 746, Issue 1, article id. 85, 24  
pp.
- Vattis Kyriakos, Koushiappas Savvas M., Loeb Abraham, 2019,  
Physical Review D, Volume 99, Issue 12, id.121302
- Vikman Alexander, 2005, Phys. Rev. D. 71(2): 023515
- Voglis C., Lagaris I.E., 2004, WSEAS International Conference on  
Applied Mathematics, Corfu, Greece
- Watson D., Denney K.D. et al., 2011, ApJ 740, L49
- Wei H., Yan X.P., Zhou Y.N., 2014, JCAP 1401, 045, 1312.1117
- Weinberg Steven, 2008, "Cosmology", Oxford University Press,  
ISBN 0191523607, 9780191523601
- Wojtak RadosÅaw, Agnello Adriano, 2019, Monthly Notices of  
the Royal Astronomical Society, Volume 486, Issue 4, p.5046-  
5051



Wood-Vasey et al., 2007, *Astrophys.J.*666:694-715, arXiv: astro-ph/0701041

Zhai A.,Blanton M., Slosar A., Tinker J., 2017, *The Astrophysical Journal*, Volume 850, Issue 2, article id. 183, 32 pp.